

# Reversible Fluorescence Quenching by Micelle Selective Benzophenone-Induced Interactions between Brij Micelles and Polyacrylic Acids: Implications for Chemical Sensors

Prasun Bandyopadhyay\* and Amit K. Ghosh

Unilever R & D Bangalore, 64 Main Road, Whitefield, Bangalore 560066, India

Received: May 17, 2010; Revised Manuscript Received: July 7, 2010

The fluorescence response of pyrene has been studied in the presence of nonionic brij micelles and poly(acrylic acid) (PAA) with benzophenone (BP) as a neutral hydrophobic quencher. Pyrene emission is quenched (“off” state) in the presence of BP in brij 35 (polyoxyethylene-23-lauryl ether) and brij 56 (polyoxyethylene-10-cetyl ether) micelles. Quenched pyrene emission is selectively recovered (“on” state) for brij 35 micelles with the addition of PAA (starting conc  $2.0 \times 10^{-5}$  M). Due to the interaction of PAA and brij 35 micelles and the relatively easier accessibility of PAA polymer chains near the bulky polyoxyethylene chain of brij 35 micelles, the chances of BP partition inside the hydrophobic polymer coil are more compared to brij 56 micelles. The PAA sensing ability of the “brij 35:pyrene:BP” system is dependent on the molecular weight ( $M$ ) of the polymer. Fluorescence recovery has been observed with PAA ( $M \sim 150000$ ) and complete recovery has been recorded with high  $M$  of PAA ( $M \sim 450000$ ); however, no fluorescence change is observed in the presence of low  $M$  of PAA ( $M \sim 2000$ ). In solution, such selective reversible fluorescence quenching has the potential for a new class of highly sensitive chemical sensor systems.

## Introduction

Surfactants and water-soluble polymers often occur together in various formulations of the chemical, biological, and pharmaceutical applications. Polymer–surfactant aggregation and interaction in solution has been studied extensively in the last few decades.<sup>1</sup> However, the interactions between nonionic surfactant and ionic polymers have attracted much less attention. In general, the interaction driving force for ionic polymer and nonionic surfactant is dominated by H-bonding and hydrophobic interactions.<sup>2</sup> This kind of interaction is controlled by the nature of the polymers, surfactants, and the environment. Interaction of polyoxyethylenic nonionic surfactant with PAA was reported for the first time by Saito and co-workers.<sup>3,4</sup> They explained the interaction of such systems as a combination of hydrophobic attraction of the apolar tail of surfactants to the backbone of PAA and H-bonding between the acidic groups of the polymer and the polar headgroup of the surfactants.<sup>5</sup> The PAA–surfactant complex is pH sensitive and occurs only in a narrow pH range. There is no complex formation above pH 5 and precipitate is formed below pH 3, which generally dissolves in the presence of excess surfactant. The surfactant concentration required to induce binding to the polymer, referred to as the critical aggregation concentration (cac), which is generally lower than the critical micelle concentration (cmc) in polymer-free solution, the difference being a measure of the strength of polymer–surfactant interaction. To study the structures on semilocal length scales in polymer–surfactant systems, several groups have used small-angle neutron scattering (SANS) to gain more insight into structural changes of the systems on molecular scales.<sup>6,7</sup>

It has been established that fluorescence techniques can provide valuable information concerning the structure of aggregate systems in aqueous solutions.<sup>8,9</sup> In this regard, pyrene and its derivatives are among the more important of the

fluorescent probes which have been used to determine properties such as the micropolarity, microviscosity, and aggregation number of many micellar systems.<sup>10</sup> Organized systems such as micelles are broadly known as microheterogeneous systems because of their colloidal dimensions, in spite of the large number of molecules they contain. Alteration of reaction rates and pathways in the environments provided by peculiar micellar properties has been recognized for a long time,<sup>11</sup> and diverse applications in different areas based on the reactivity control exerted by these systems have been developed.<sup>12</sup> Particularly, nonionic micelles have been proved to enhance molecular recognition in chemosensing systems.<sup>13</sup> It has remained a challenge to incorporate the sensitivity and selectivity offered by ligand/receptor interactions into sensors that can be extremely sensitive, robust, and versatile.

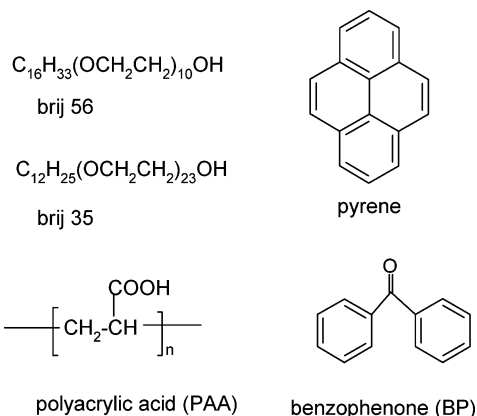
To the best of our knowledge, exploitation of the structural effect of nonionic surfactant toward its interaction with PAA to develop a potential chemical (here PAA) sensor by fluorescence probe investigation was not reported. In this paper, we propose for the first time a model of the fluorescent supramolecular chemosensor “brij35:pyrene:BP”. The sensing ability of this system is dependent on the molecular weight of the PAA analyzed; in general, the higher the  $M$  of PAA, the greater is the interaction with brij surfactant and thus the higher is the sensing ability.

The idea was to use a hydrophobic quencher like BP both as a potential binder to nonionic micelles and to partition in hydrophobic polymer chain depending on its close proximity. We have harnessed the polymer–surfactant interaction in the presence of pyrene and BP to demonstrate this potential new class of highly sensitive chemical sensor systems.

## Experimental Section

**Materials.** PAA (molecular weight 2000, 150000, and 450000 Da), benzophenone, and brij surfactants (Scheme 1) were procured from Sigma-Aldrich Chemicals Co. (St. Louis, MO), and pyrene was purchased from Fluka. Water was

\*To whom correspondence should be addressed. E-mail: prasun.bandyopadhyay@unilever.com. Phone: +91-080-39830992. Fax: 091-080-2845-3086.

**SCHEME 1: Molecular Structure of brij 56, brij 35, Pyrene, Polyacrylic Acid, and Benzophenone**

obtained from a Milli-Q purification system. All experiments were performed with freshly prepared solutions. In order to ensure equilibrium, measurements were conducted after 24 h of storage at room temperature.

**Fluorescence Studies.** All fluorescence studies were performed using a Shimadzu RF-5301PC spectrofluorophotometer. Stock solutions of pyrene ( $1 \times 10^{-3}$  M) were prepared in ethanol, and the final concentration of pyrene was fixed at  $9 \times 10^{-8}$  M for all studies. The excitation wavelength was set at 340 nm. The first vibronic band ( $I_1$ ) and the third ( $I_3$ ) vibronic band of the emission spectrum of pyrene were monitored at 373 and 384 nm, respectively. The excitation and emission slit widths were set at 3 and 5 nm, respectively. Stock solutions of benzophenone ( $27 \times 10^{-3}$  M) were prepared in ethanol and then diluted in MQ water for all studies. The final pH of the solution was maintained between 3 and 4.

**pH Measurement.** pH measurements were performed by means of a control dynamic pH meter.

**Turbidimetry.** The turbidimetric measurement and pyrene absorbance studies were performed using a Perkin-Elmer Lambda 35 UV/vis spectrophotometer. A wavelength of 400 nm in the visible regime was selected to examine all solutions. The spectrum was taken in transmittance ( $T\%$ ) mode to maximum precision. Measurements were carried out on two or three sample solutions prepared at different times from the same materials (replicates).

**DLS Measurements.** DLS measurements were performed on a Brookhaven Instrument (BI 2000) equipped with an autocorrelator (BI-9K) and goniometer (BI-200SM) with a BIHV photomultiplier tube. An argon ion laser (LEXEL 95-2) operating at 488 nm was used as a light source. The beam was focused onto the sample cell (standard cylindrical 4.5 mL cuvettes) through a temperature-controlled chamber (the temperature was controlled within  $23 \pm 0.1$  °C). All experiments were done at a correlation time of 2 min. The measurements were carried out at 90°. The available software records the autocorrelation of the intensity trace during the experiment. Once the autocorrelation data have been generated, the averaged translational diffusion coefficient of the protein samples is derived mathematically from the fitting parameter, the average decay rate, and the scattering vector at a given angle of 90°. The hydrodynamic radius,  $R_H$ , is computed on the basis of the Stokes–Einstein equation. Three measurements were taken for each system, and then, the average hydrodynamic radius was obtained.

**Conductance Measurement.** The conductivity measurement was performed by using a control dynamics (APX 185)

**TABLE 1: Parameter Obtained from Fluorescence and Fluorescence Quenching Experiments for PAA ( $M \sim 450000$ )**

surfactant	cac ( $10^{-6}$ M)	cmc ( $\times 10^{-6}$ M)	cac/cmc	$N_A$	$K_{SV}$ ( $M^{-1}$ )
brij35	80	160	0.50	38	$2.8 \times 10^4$
brij56	15	19	0.78	100	$1.9 \times 10^4$

conductivity meter. The measuring probe has been calibrated with saline solutions of known conductivity and permittivity.

**Results and Discussion**

**Steady-State Fluorescence Quenching Study in Micellar Environments.** In the micellar medium, there are two factors that affect the mutual counter of the probe and the quencher molecules. These are (i) the partitioning of the fluorescent probe and the quenchers between the micellar and aqueous phases and (ii) the dynamic distribution of the quenchers and the fluorescent probe during the quenching process.

The steady-state fluorescence quenching experiment using quencher is an established technique to assess the accessibility of a fluorophore toward the quencher molecule in a micellar environment.<sup>14,15</sup> A relative measure of the quenching efficiency ( $K_{SV}$ ) reflects the accessibility of one to the other. Thus, such studies can throw light on the approachability of the quencher to the fluorophore, i.e., the compactness of the micellar head groups. The surfactant concentrations were maintained much above the cmc for both cases, and they are  $180 \times 10^{-6}$  and  $50 \times 10^{-6}$  M for brij 35 and brij 56, respectively. In this condition, the excimer emission is only feeble; thus, quenching of the pyrene monomer emission with two surfactant systems by BP was monitored. The Stern–Volmer constants ( $K_{SV}$ ) were determined (Table 1) using the Stern–Volmer equation, which can be expressed as follows:

$$F_0/F = 1 + K_{SV}[Q] \quad (1)$$

$F_0$  and  $F$  are the fluorescence intensities of pyrene monomer in the absence and presence of different concentrations of the quencher.  $K_{SV}$  and  $[Q]$  are the Stern–Volmer constant and quencher concentration, respectively.

BP has quenched the fluorescence of pyrene in the presence of brij micelles. The plot of  $F_0/F$  vs quencher concentration is linear (Figure 1a) in both brij micelles, indicating only one quenching mechanism is operating, either static or dynamic. In order to identify the quenching mechanism as being dynamic or static, fluorescence quenching data were collected at different temperatures.<sup>8</sup> For this purpose, the pyrene fluorescence spectra in the presence of brij 35 micelles were recorded without and with various concentrations of BP at different temperatures (25, 45, and 65 °C). Stern–Volmer plots obtained from this data are collected in Figure 1b. It can be seen that the quenching efficiency correlates inversely with temperature, strongly supporting the static mode of quenching.<sup>8</sup> The quenching efficiency (Stern–Volmer constant) has reduced 5 times (from  $2.8 \times 10^4$  to  $0.56 \times 10^4$   $M^{-1}$ ) as the temperature increased from 25 to 65 °C. The increase in temperature lowers the stability of weak “pyrene–BP” conjugate formation, thereby reducing the fluorescence quenching efficiency. To gather further support for the proposed quenching mechanism, the absorption spectrum of pyrene was monitored with and without BP, as shown in the Supporting Information, Figure S-1. It is apparent that the absorption maximum of pyrene shows a red-shift with increase in intensity upon addition of BP. This confirms the static

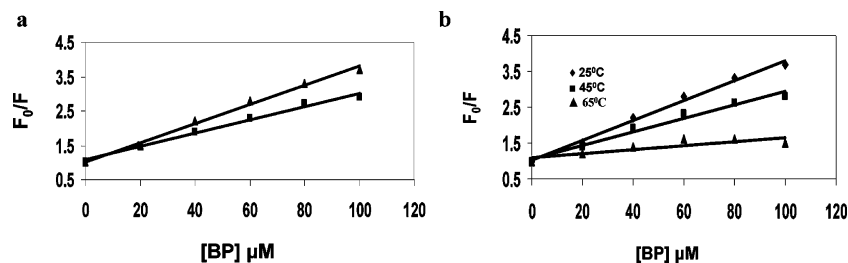


**Figure 1.** (a) Stern–Volmer plots for the pyrene fluorescence quenching upon addition of benzophenone in the presence of brij 35 (▲) and brij 56 (■). (b) Stern–Volmer plots of pyrene fluorescence quenching upon addition of benzophenone in the presence of brij 35 at different temperatures. PAA used  $M \sim 450000$ .

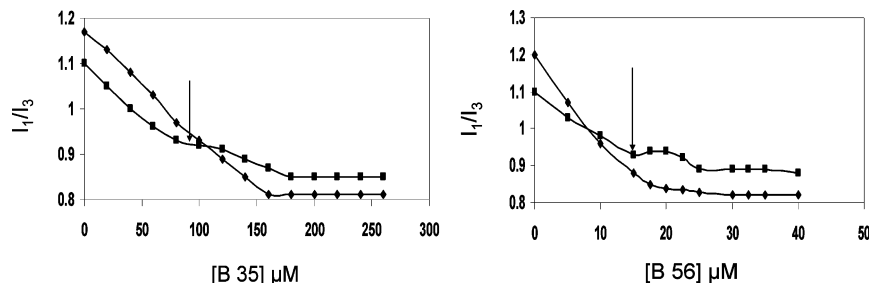


**Figure 2.** Changes in the  $I_1/I_3$  intensity ratio of the pyrene emission as a function of surfactant concentration, in the presence (■) and absence (◆) of PAA; the arrow indicates the critical aggregation concentration (cac) of surfactant in the presence of polymer. PAA used  $M \sim 450000$ . [B35] = concentration of brij 35 surfactant, and [B56] = concentration of brij 56 surfactant.

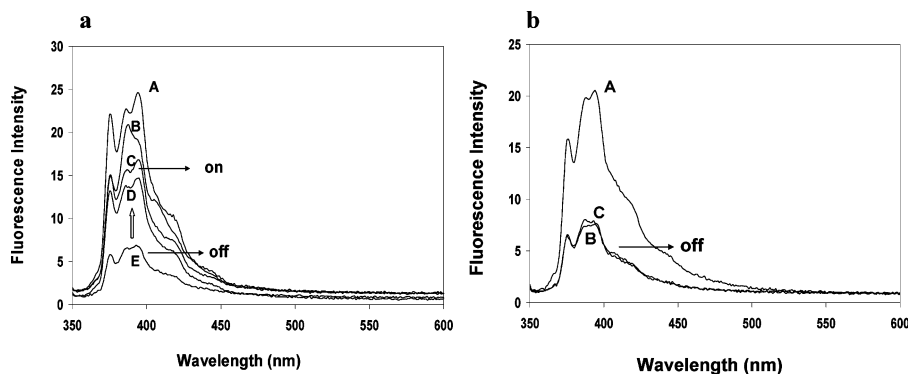


**Figure 3.** (a) Emission spectra of (A) pyrene ( $9 \times 10^{-8}$  M) in the presence of brij 35 ( $150 \times 10^{-6}$  M), (E) pyrene:brij 35 micelle:BP, and "pyrene:brij 35 micelle:BP" in the presence of (D)  $2.0 \times 10^{-5}$  M PAA, (C)  $5 \times 10^{-5}$  M PAA, and (B)  $6.5 \times 10^{-5}$  M PAA. (b) Emission spectra of (A) pyrene ( $9 \times 10^{-8}$  M) in the presence of brij 56 ( $50 \times 10^{-6}$  M), (B) pyrene:brij 56 micelle:BP, and (C) "pyrene:brij 56 micelle:BP" in the presence of  $2.0 \times 10^{-5}$  to  $7.8 \times 10^{-5}$  M PAA. PAA used in all experiments,  $M \sim 450000$ .

quenching mechanism and suggests that a new weak complex between "pyrene and BP" is formed with different electronic structure.<sup>8</sup>

BP quenching was quite effective (high  $K_{SV}$  value) at low surfactant concentrations, but as the surfactant concentration increases much above the cmc, quenching becomes less effective (low  $K_{SV}$  value). Increased surfactant concentration may facilitate the partitioning of pyrene in micellar nanocages. At surfactant concentrations just above the cmc, however, some pyrene molecules are left unprotected in the aqueous phase and are easily quenched by BP. Generally, the number of micelles increases with increasing surfactant concentration, resulting in a higher fraction of pyrene molecules residing inside the micellar pseudophase. Above cmc, the  $K_{SV}$  value for brij 35 is estimated to be slightly higher than that for brij 56. The aggregation number of the nonionic surfactant micelles monotonically decreases with increasing polyoxyethylene chain length. The aggregation numbers reported for brij 56 and brij 35 are 100 and 38, respectively.<sup>16,17</sup>

**Physicochemical Properties of brij Micelles and the Effect of PAA ( $M \sim 450000$ ).** The fluorescence value of pyrene  $I_1/I_3$  is very sensitive to the polarity of the microenvironment. When

surfactant molecules aggregate, pyrene is solubilized in the hydrophobic part of the aggregates and  $I_1/I_3$  decreases. Figure 2 shows the dependence of the  $I_1/I_3$  on the brij surfactant concentration in the presence and absence of PAA. The cmc and cac values are listed in Table 1. The decrease in  $I_1/I_3$  reflects the low polarity of the pyrene microenvironment.

The strength of the interaction between polymer and surfactant can be characterized by the semiquantitative cac/cmc ratio.<sup>18</sup> Polymer–surfactant interaction is stronger when the value of the cac/cmc ratio is small, which could be the reason for the lower cac/cmc value for brij 35 as compared to brij 56.

As shown in Figure 3a, addition of PAA to solutions of BP quenched pyrene in brij 35 micelles results in recovery of its fluorescence. Addition of a very low concentration ( $2.0 \times 10^{-5}$  M) of PAA starts the fluorescence recovery; this could be due to the higher chances of BP partitioning in PAA coil. The greater the chances of interaction of PAA chain with polyoxyethylene chain, the higher the possibility of BP partitioning in PAA coil. It is expected that PAA interaction with brij 56 micelles (shorter polyoxyethylene chain [ $n = 10$ ] and longer hydrophobic chain [ $n = 16$ ]) would be weaker compared to brij 35 micelles (longer polyoxyethylene chain [ $n = 23$ ] and shorter hydrophobic chain

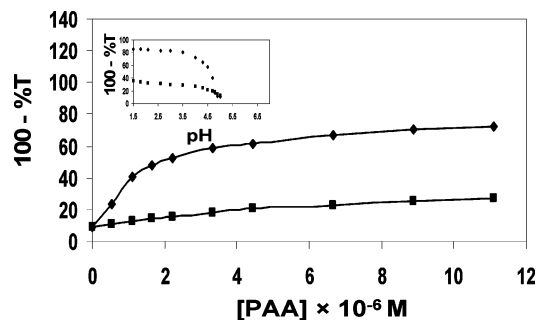


**Figure 4.** Turbidimetric plots for interaction of brij surfactant (■ brij 56, ◆ brij 35) micelles and PAA. Inset: pH turbidimetric titration of PAA (2.5 mM,  $M \sim 450000$ ) and brij surfactant (■ brij 56, ◆ brij 35) micelles, at constant ionic strength.

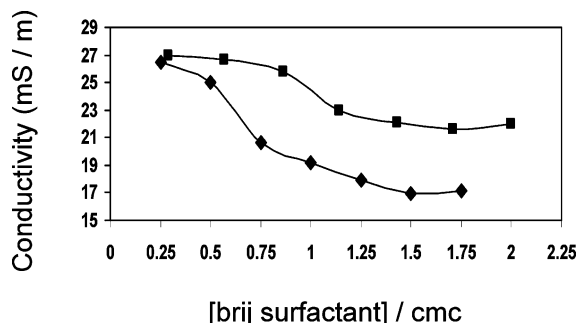


**Figure 5.** Conductivity plots for interaction of brij surfactant (■ brij 56, ◆ brij 35) micelles and PAA ( $M \sim 450000$ ).

[ $n = 10$ ]). The lesser the chances of interaction of the PAA chain with the brij micelle, the lower is the possibility of BP permeation inside the PAA polymer coil.

In fact, no fluorescence intensity change occurs when the same amount of PAA is added to the BP quenched pyrene sample of brij 56. Even in the presence of a much higher concentration of PAA addition ( $7.8 \times 10^{-5}$  M) is unable to recover fluorescence emission, where it mostly remains as quenched form (Figure 3b). This could be due to inaccessibility of PAA polymer coil near BP in brij 56 micelles.

The levels of PAA “sensed” by the recovery of pyrene fluorescence for the brij 35 micellar system are quite low ( $2.0 \times 10^{-5}$  M). The system described above is remarkable from a number of different perspectives. The key component is the pyrene in the hydrophobic environment of the nonionic micelle, quenched by BP, which leads to some critical effects. First is the quenching sensitivity, which proves the close proximity of pyrene and loosely bound BP present in the micelle (“off” state). Second, once the quenching reagent (here BP) has been stripped

away by the PAA polymer coil, the BP entangled PAA polymer chain leads to strong fluorescence recovery (“on” state).

However, this could be an artifact of “pyrene interaction with PAA polymer coil in brij 35”. To test this possibility and confirm our hypothesis, we have performed similar fluorescence experiment without addition of BP. The result shows *no fluorescence intensity change* after addition of polymer (Supporting Information, Figure S2) in the pyrene encapsulated brij 35 system, which strengthens our hypothesis about “BP stripping in PAA polymer coil” in the presence of brij 35.

We have studied the interaction of PAA with brij 35 and brij 56 by turbidity, conductivity, and DLS (dynamic light scattering) measurements to reconfirm the extent of PAA–brij micelle (brij 35 vs brij 56) complex formation. The turbidimetric plots for the brij micelles and PAA are shown in Figure 4. In the case of brij 35, the turbidity values as given by the ( $100 - T$  %) increases steeply compared to brij 56, proving the higher degree of interaction of PAA with brij 35. To study the pH effect on PAA and brij micelle interaction, “pH” turbidimetric titrations were conducted by adding HCl to 2.5 mM PAA and brij micelle mixture in the presence of 0.1 M NaCl (Figure 4). The pH of the solution increases as a result of H-bonding between PAA and ether oxygen atoms of the brij surfactants. The interaction is enhanced for the case of brij 35 due to its longer polyoxyethylene chain. In both cases, complex formation appears to be reversible by addition of NaOH to the turbid solution. This is consistent with Saito’s report that protons of the carboxyl group of PAA are fixed due to H-bonding interactions between PAA and polyoxyethylene type nonionic surfactant under acidic conditions.<sup>19</sup> Figure 5 shows the effect of brij surfactant on the electrical conductivity of the PAA/water system, keeping the polymer concentration constant. The conductivity significantly decreases by increasing the brij 35 surfactant concentration and has plateaus at low and respectively higher concentration level. The conductivity of the solution decreases as a result of H-bonding between PAA and ether oxygen atoms of the brij surfactants. The interaction is enhanced for the case of brij 35 due to the longer polyoxyethylene chain, as indicated by the lower conductivity value compared to the brij 56 containing system. DLS measurement confirms the assembly of the PAA–brij 35, where the hydrodynamic radius increases compared to the PAA–brij 56 aggregate (Figure 6). These results clearly indicate that the larger the size of polyoxyethylene chains, the higher the chances of interaction between the PAA chain and polyoxyethylene group of brij surfactant.

On the basis of these results, we propose, in the case of brij 35, more PAA chains will enter in polyoxyethylene chains and strip away BP in its polymer coil. Thus, pyrene fluorescence will be reversed back due to lack of quencher in its vicinity,

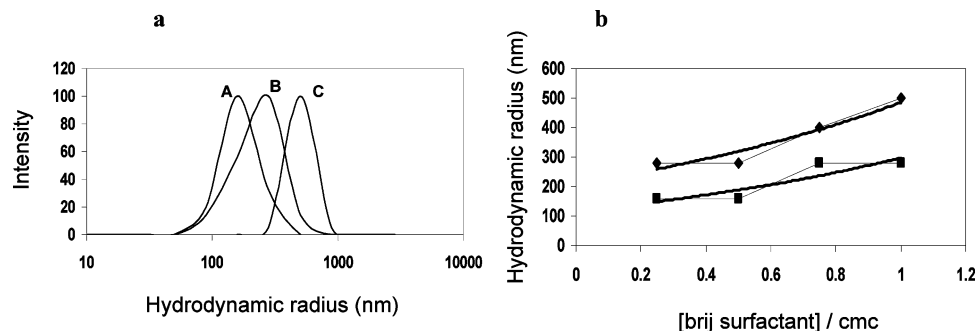


**Figure 6.** (a) DLS signals of (A) 10  $\mu$ M PAA, (B) PAA with brij 56, and (C) PAA with brij 35. In both cases, the surfactant concentration was kept above the cmc. (b) Hydrodynamic radius of PAA–brij micelle aggregates (■ brij 56, ◆ brij 35). PAA used in all experiments,  $M \sim 450000$ .



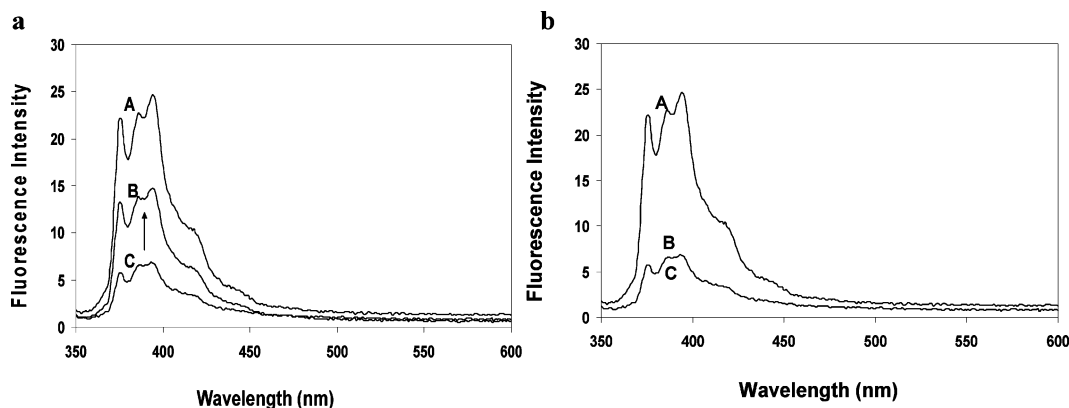


**Figure 7.** (a) Emission spectra of (A) pyrene ( $9 \times 10^{-8}$  M) in the presence of brij 35 ( $150 \times 10^{-6}$  M), (C) pyrene:brij 35 micelle:BP, and (B) “pyrene:brij 35 micelle:BP” in the presence of  $6.5 \times 10^{-5}$  M PAA ( $M$  150000). (b) Emission spectra of (A) pyrene ( $9 \times 10^{-8}$  M) in the presence of brij 35 ( $150 \times 10^{-6}$  M), (C) pyrene:brij 35 micelle:BP, and (B) “pyrene:brij 35 micelle:BP” in the presence of  $7.8 \times 10^{-5}$  M PAA ( $M$  2000).

**SCHEME 2: Proposed Fluorescence Quenching and Recovery Mechanism: Location of Quenched Pyrene (Dark Yellow), Fluorescent Pyrene (Green), and BP (Blue) in (A) brij 35 Micelle and (B) brij 56 Micelle**

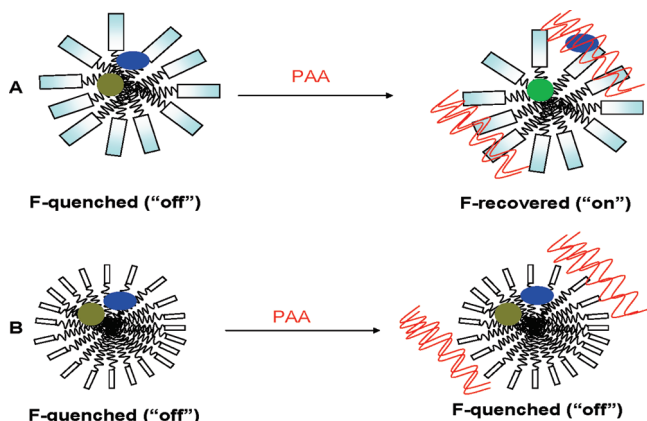


**TABLE 2: Parameter Obtained from Fluorescence Experiments by Varying the Molecular Weight of PAA**

surfactant	cac ( $10^{-6}$ M)	cmc ( $\times 10^{-6}$ M)	cac/cmc	PAA (molecular weight)
brij35	80	160	0.50	$\sim 450000$
	120		0.75	$\sim 150000$
	140		0.87	$\sim 2000$
brij56	15	19	0.78	$\sim 450000$
	16		0.84	$\sim 150000$
	18		0.94	$\sim 2000$

i.e., “off” to “on” state. This is not possible for brij 56 micelle where the probability of PAA accessibility toward brij 56 micelle is less, resulting in limited chances of stripping away of BP in the PAA hydrophobic pocket (Scheme 2).

To confirm the selectivity toward PAA polymer sensing, we have conducted control experiments with carboxy methyl cellulose (CMC). No fluorescence recovery has been observed, indicating CMC has almost “no or very weak interaction” with brij surfactants (Supporting Information, Figure S3).

**Effect of PAA Molecular Weight toward Surfactant cmc and Sensing Ability.** The effect of PAA molecular weight ( $M$ ) toward the cmc of brij 35 and brij 56 has been studied in detail. The cac values with varying  $M$  of PAA polymer are listed in Table 2. The data clearly shows that with increasing  $M$  of the polymer the cac value decreases, indicating stronger polymer–surfactant interaction. Polymer–surfactant interaction is stronger

when the value of the cac/cmc ratio is small. Supporting Information Figures S3–S6 show a decrease in  $I_1/I_3$  values in the presence of PAA ( $M$  150000 and 2000) toward determination of the cac values of brij 35 and brij 56 surfactants.

The PAA sensing ability of the “brij 35:pyrene:BP” system is dependent on  $M$  of the polymer. Fluorescence recovery has been observed with PAA ( $M \sim 150000$ ) and complete recovery has been recorded with high  $M$  of PAA ( $M \sim 450000$ ); however, no fluorescence change is observed in the presence of low  $M$  of PAA ( $M \sim 2000$ ) (Figure 7). This could be due to greater chances of complex formation of PAA with brij 35 with increasing  $M$ . The higher the PAA coil accessibility toward brij micelles, the greater the chances of BP stripping inside the PAA coil and thus the higher the chances of fluorescence recovery. In high  $M$ , a polymer coil can accommodate more than one micelle. Since the polymer coil can accommodate several micelles, the maximum amount of polymer-bound surfactant becomes proportional to the mass concentration of polymer. It has also been reported in the literature<sup>20</sup> that chances of polymer complex formation with micelle increase with increasing molecular weight of polymer.

## Conclusions

In summary, (1) we have shown that the polyoxyethylene headgroup of brij surfactant plays an important role in the PAA–brij micelle interaction. The polyoxyethylene groups (23 in brij 35 and 10 in brij 56) make the interaction between brij 35 micelles with PAA stronger compared to brij 56 micelles and PAA. (2) On the basis of this interaction difference, we have developed a supramolecular chemosensor system “brij35:pyrene:BP” which can sense PAA based on polymer–micelle interaction. (3) In the presence of micelles, BP quenches pyrene fluorescence through a static mode of action by forming a nonfluorescing complex. (4) The BP quenched emission is completely recovered with the addition of a very low concentration of PAA ( $M \sim 450000$ ), due to stripping of BP in the PAA polymer coil. (4) These results can be used to design and improve fluorescent “chemical” sensors of high sensitivity and selectivity.

**Acknowledgment.** We thank the reviewers for the constructive criticisms and valuable suggestions of the work.

**Supporting Information Available:** Absorbance spectra of pyrene in the presence/absence of BP, fluorescence spectra for

control experiments,  $I_1/I_3$  vs surfactant concentration plot for various PAA molecular weights, and comparative cac/cmc data from conductivity and fluorescence measurements. This material is available free of charge via the Internet at <http://pubs.acs.org>.

## References and Notes

- (1) Goddard, E. D.; Ananthapadmanabhan, K. P., Eds. *Interaction of Surfactants and Polymers and Proteins*; CRC Press: Boca Raton, FL, 1993.
- (2) Robb, I. D.; Stevenson, P. *Langmuir* **2000**, *6*, 7168–7172.
- (3) Saito, S.; Taniguchi, T. *Kolloid Z. Z. Polym.* **1971**, *248*, 1039–1040.
- (4) Saito, S. In *Nonionic Surfactants, Physical Chemistry*; Schick, M. J., Ed.; Surfactant Sciences Series, Vol. 23; Marcel Dekker: New York, 1987; Chapter 15.
- (5) Saito, S. *J. Am. Oil Chem. Soc.* **1989**, *66*, 987–993.
- (6) Sommer, C.; Pedersen, J. S.; Garamus, V. M. *Langmuir* **2005**, *21*, 2137–2149.
- (7) Bu, H.; Kjoniksen, A.-L.; Knudsen, K. D.; Nystrom, B. *Colloids Surf., A* **2007**, *293*, 105–113.
- (8) Lakowicz, J. R. *Principles of Fluorescence Spectroscopy*; Plenum: New York, 1999.
- (9) Bandyopadhyay, P.; Saha, K. *Chem. Phys. Lett.* **2008**, *457*, 227–231.
- (10) Turro, N. J.; Arora, K. S. *Polymer* **1986**, *27*, 783–789.
- (11) Fendler, J. H.; Fendler, E. J. *Catalysis in Micellar and Macromolecular Systems*; Academic Press: New York, 1975.
- (12) Guo, L.; Liang, Y. *Can. J. Chem.* **2002**, *80*, 1655–1661.
- (13) Niihara, K.; Anslyn, E. V. *J. Org. Chem.* **2003**, *68*, 10156–10157.
- (14) Bandyopadhyay, P.; Bandyopadhyay, S.; Ghosh, A. K. *Chem. Phys. Lett.* **2009**, *476*, 244–248.
- (15) Bandyopadhyay, P.; Ghosh, A. K. *J. Phys. Chem. B* **2009**, *113*, 13462–13464.
- (16) Sulthana, S. B.; Rao, P. V. C.; Bhat, S. G. T.; Nakao, T. Y.; Sugihara, G.; Rakshit, A. K. *Langmuir* **2000**, *16*, 980–987.
- (17) Becher, P. *J. Colloid. Sci.* **1961**, *16*, 49–56.
- (18) Shirahama, K.; Idle, N. *J. Colloid Interface Sci.* **1976**, *54*, 450–452.
- (19) Saito, S.; Schick, M. J., Eds. *Nonionic Surfactants, Physical Chemistry*; Surfactant Sciences Series, Vol. 23; Marcel Dekker: New York, 1987; Chapter 15.
- (20) Meszaros, R.; Varga, I.; Gillanya, T. *J. Phys. Chem. B* **2005**, *109*, 13538–13544.

JP104463U